

# Internally excited acoustic resonator for photoacoustic trace detection

Sorasak Danworaphong, Irio G. Calasso, Andrew Beveridge, Gerald J. Diebold, Claire Gmachl, Federico Capasso, Deborah L. Sivco, and A. Y. Cho

The quantum-cascade laser can be used as an infrared source for a small portable photoacoustic trace gas detector. The device that we describe uses a quantum-cascade laser without collimating optics mounted inside an acoustic resonator. The laser is positioned in the center of a longitudinal resonator at a pressure antinode and emits radiation along the length of the resonator exciting an axially symmetric longitudinal acoustic mode of an open-ended cylindrical resonator. Experiments are reported with an 8- $\mu\text{m}$ , quasi-cw-modulated, room-temperature laser used to detect  $\text{N}_2\text{O}$ . © 2003 Optical Society of America

OCIS code: 300.6430.

## 1. Introduction

Perhaps the most successful application of the photoacoustic effect<sup>1–5</sup> has been for trace detection of gases. The detection limit of a photoacoustic detector consisting of an acoustic resonator, a microphone, an amplitude-modulated continuous laser, and a lock-in amplifier is typically in the parts per billion range; at the same time, the dynamic range of the instrument can easily be over one million. The selectivity of the photoacoustic effect, where a narrow-band laser excites only those species with absorptions at the laser wavelength, is also a valuable feature of the photoacoustic effect in its application to trace detection. Since the first reports<sup>6–8</sup> of use of CO and CO<sub>2</sub> lasers to generate the photoacoustic effect in gases, high-power, continuous lasers have been the radiation source of choice for the production of the photoacoustic effect in the infrared. Such lasers typically produce a collimated beam of radiation with an output of the order of 1 W, which can be directed into a cylindrical acoustic cell and modulated at the res-

onance frequency of an acoustic mode of the cell, increasing the amplitude of the photoacoustic effect by an amount proportional to the quality factor of the resonator and greatly enhancing the capability of the device for trace detection.

In practice, the magnitude of the photoacoustic effect in gases is so large that in typical devices the overall detection limit is limited not by the noise of the microphone but by a small extraneous acoustic signal, referred to as the “window” signal, generated by absorption of radiation at the entrance and exit windows of the cell.<sup>6,8,9</sup> Over the years, a number of resonator designs have been employed to reduce the magnitude of the window signal through use of baffles to block the acoustic signal generated at the window from reaching the microphone or through design of the acoustic resonator so that the points of entrance and exit of the laser beam in the cell are at acoustic nodes of the resonator, thereby nullifying the contribution of the window signal to the mode of the resonator excited by the optical excitation. A review of the various resonator designs used to optimize detection limits has been given by Sigrist in Ref. 10. Generally speaking, it can be said that, even before the invention of the laser, the design of photoacoustic resonators has been dictated to a large extent by the characteristics of the radiation source.

The quantum-cascade laser<sup>11,12</sup> has been shown to be admirably suited to gas phase absorbance measurements and trace detection in the near infrared.<sup>13–17</sup> Photoacoustic trace detection has been reported with a cryogenically cooled quantum-cascade laser<sup>18</sup> in a device where the output of the

---

S. Danworaphong is with the Department of Physics, Brown University, Providence, Rhode Island 02912. I. G. Calasso, A. Beveridge, and G. J. Diebold (gerald\_diebold@brown.edu) are with the Department of Chemistry, Brown University, Providence, Rhode Island 02912. C. Gmachl, F. Capasso, D. L. Sivco, and A. Y. Cho are with Lucent Technologies, Bell Laboratories, 600 Mountain Avenue, Murray Hill, New Jersey 07974.

Received 23 October 2002; revised manuscript received 18 July 2003.

0003-6935/03/425561-05\$15.00/0

© 2003 Optical Society of America

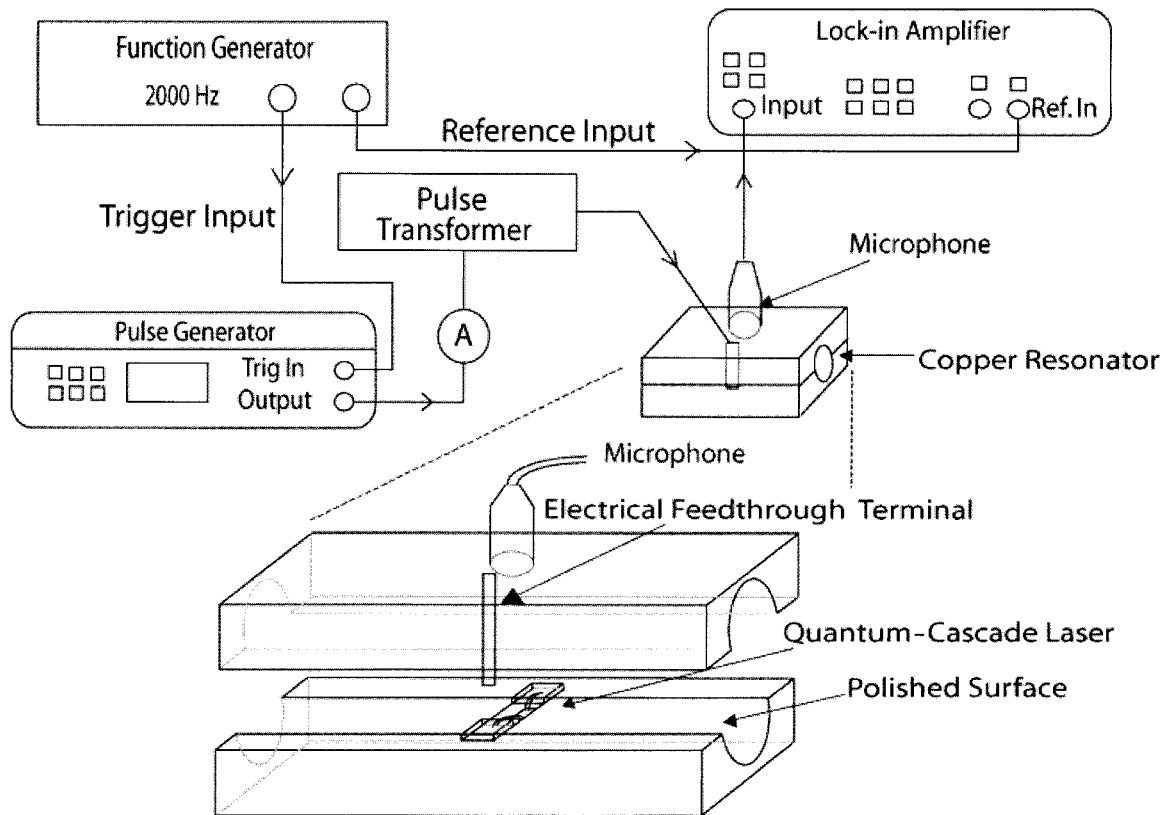


Fig. 1. Diagram of the experimental apparatus. The pulse generator delivers 83.4-kHz, 50-ns pulses to the quantum-cascade laser, which is amplitude modulated at 2 kHz by the function generator. Trig, trigger; Ref., reference.

laser was collimated and directed into a photoacoustic resonator. Cryogenic cooling boosts the output power of the laser, but detracts substantially from the field portability of a photoacoustic trace detector. Here we describe use of a quantum-cascade laser for photoacoustic trace detection. The resonator design incorporates a laser placed inside the acoustic resonator and uses the radiation emitted from both ends of the laser chip to excite a longitudinal acoustic resonance in an open tube. The laser beam, as a result of its inherently large beam divergence, undergoes multiple reflections off of the internal surfaces of the acoustic cavity filling the volume of the resonator. Unlike conventional photoacoustic resonator designs where absorption of the laser beam at the window surfaces determines the detection limits, absorption of the laser beam on reflection from the internal surfaces of the resonator is sufficiently small that it does not provide the dominant source of noise; rather, it is the intrinsic noise of the microphone that governs the theoretical detection limit at the power levels of the laser used here. Experimental results for operation of the device as an atmospheric pressure trace detector of  $N_2O$  at  $8 \mu\text{m}$  are reported.

## 2. Experiments

The theory of photoacoustic excitation of an open-ended cylindrical resonator has been given by several authors.<sup>19–23</sup> The pressure response of the resona-

tor is obtained through solution of the wave equation for pressure, which follows from the coupled equations for temperature and pressure in the limit of negligible heat conduction. The properties of a cylindrically symmetric, longitudinal resonator have been given in Refs. 24 and 25. The magnitude of the photoacoustic pressure  $p$  for a longitudinal resonator driven at its resonance frequency  $f$ , according to Ref. 24, is given by

$$p = \alpha l W_L Q \frac{(\gamma - 1)}{2\pi f V}, \quad (1)$$

where  $\alpha$  and  $\gamma$  are the optical absorption coefficient and heat capacity ratio for the gas, respectively;  $W_L$  is the laser power;  $V$  and  $l$  are the volume and length of the cell, respectively; and  $Q$  is the quality factor of the resonance. An analysis of the dissipative factors of the cell show that the quality factor increases with the radius of the resonator  $r$ , so the acoustic pressure scales as the inverse of the radius.

The open-ended windowless resonator used in the experiments was fabricated from a copper block 85 mm long, 50 mm wide, and 38 mm high as shown in Fig. 1. The copper block was constructed so that various-diameter polished tubes could be mounted inside. It was thus possible to determine the detection limits with acoustic resonators with varying radii but with the same length and same overall laser

power. A Bruel and Kjaer 0.50-in. (–1.27-cm) condenser microphone, Model 4130, was placed at the center of the resonator directly above the quantum-cascade laser at a pressure antinode of the resonator. The channel for the microphone leading into the interior of the resonator was approximately the same diameter as the microphone diaphragm. The quantum-cascade laser chip was attached to a copper plate, which, in turn, was mounted on an interior surface of the cell located at the center of the resonator. The laser was fabricated to emit radiation at two surfaces on opposite ends of the chip so that radiation filled the resonator in both directions from the center of the resonator. The laser, which was elevated a few millimeters above the bottom of the resonator channel, was positioned at the center of the resonator with the copper block forming one electrode and an insulated pin fed through the upper copper block forming the second. The resonator design, with both the laser and the microphone located at a velocity node, which is a pressure antinode of the resonator, as well, is perhaps an optimum placement for these two components, providing only a small perturbation of the longitudinal resonance. The construction of the cell was such that heat generated by the laser, operated without an external cooling source, was dissipated by conduction to the base of the cell. A Hewlett-Packard Model 8114A pulse generator whose output was fed to an Avtech, Inc. Model AVX-M3 pulse transformer drove the quantum cascade at 83.4 kHz with 50-ns square pulses. The output of the pulse generator, in turn, was square-wave modulated at the resonance frequency of the acoustic cavity, 2 kHz, by an external function generator. The maximum voltage and current at the pulser output before the step-down transformer was 50 V and 1.5 A, respectively. The signal from the microphone was fed without further amplification to a two-channel lock-in amplifier.

The laser operated at  $1248\text{ cm}^{-1}$  with a bandwidth of  $1\text{ cm}^{-1}$  at room temperature. We determined the laser power by first calibrating a Fermionics, Inc. Model PV-12-1-T liquid-nitrogen-cooled HgCdTe detector. A 1-W  $\text{CO}_2$  laser beam was directed through a ZnSe lens and pinhole, and its power was measured with a conventional thermopile laser powermeter at a point where the expanded beam filled the face of the detector. The beam profile of the expanded laser beam beyond the focal point of the lens was then determined by use of a liquid-crystal sheet. Next, the HgCdTe detector was placed in the expanded laser beam together with calibrated attenuators, and its output voltage was recorded. With these measurements it was possible to calibrate the intensity response of the HgCdTe detector (volts per watt) at an intensity low enough so as not to exceed the linear range of the detector. The beam profile of the quantum-cascade laser was determined by scanning the laser across the face of the HgCdTe detector. The quantum-cascade laser output power was determined from a knowledge of its beam profile and the signal from the HgCdTe detector, corrected for its

spectral response. The quantum-cascade laser was found to emit a time-averaged total power of  $10\text{ }\mu\text{W}$  on each face.

The detection limit of the resonator was determined with  $\text{N}_2\text{O}$  at 1 atm. The absorption coefficient of  $\text{N}_2\text{O}$  at 1 atm was determined by placing a 10-cm-long absorption cell equipped with NaCl windows between the quantum-cascade laser and the HgCdTe detector. The transmission of the cell was recorded with a series of gas mixtures of  $\text{N}_2\text{O}$  diluted in Ar at mole fractions from 0.2 to 1. The figure obtained for the extinction coefficient,  $0.17\text{ cm}^{-1}$  at 1 atm, corresponds to the absorption of the gas without consideration of linewidth, the mode structure, or the exact wavelength of the laser relative to the absorption maximum of the  $\text{N}_2\text{O}$ ; although the extinction coefficient is not transferable to other infrared sources, it provides an integrated absorption coefficient characteristic of the spectral emission profile of the laser used here and permits determination of a photoacoustic detection limit.

The measurements were performed in neat  $\text{N}_2\text{O}$  by filling the resonator in an acoustically isolated container by recording the signal from the lock-in amplifier at the frequency where the signal amplitude was at its maximum. The sound speed in  $\text{N}_2\text{O}$  is 263 m/s, which is somewhat lower than that in air, so the modulation frequency of the laser was adjusted correspondingly downward so that the resonator was operated on resonance. With the resonator filled with Ar, a plot of the microphone signal from the lock-in amplifier versus the driving voltage on the quantum-cascade laser showed a gradual increase in signal with increasing drive voltage from the pulse generator even before the lasing threshold was reached, indicating that the background signal in the cell was electrical and did not arise from absorption of laser radiation at the resonator walls; hence, it follows that the equivalent of the window signal in a conventional photoacoustic detector, which is absorption of the laser radiation at the walls of the cell in the present experiments, cannot be considered the primary factor in the determination of the detection limit. With the laser operating above threshold, the electrical pickup seen in the lock-in amplifier was 3.5 mV. No efforts were made to reduce the electrical pickup, although minor modification of the electrical feedthrough from the pulse generator or a modification of the shielding of the microphone would be expected to reduce the electromagnetic coupling between the pulse generator and the microphone. Electrical pickup can be reduced by proper design of the electrical feedthroughs into the quantum-cascade laser and is not considered a fundamental limitation on the detection limit of the device. The intrinsic noise of the microphone and electronics, insofar as this study is concerned, constitutes a source of noise that cannot be eliminated and hence determines the theoretical limit for photoacoustic detection.<sup>26</sup> The internal noise in the microphone was determined through a turning off of the pulse generator and recording the noise in the microphone in an acoustical

**Table 1. Quality Factors and Detection Limits for Three Resonators**

Resonator Diameter (cm)	Quality Factor	Detection Limit
1.0	26	$9.4 (\pm 0.3) \times 10^{-10} \text{ cm}^{-1} \text{ W}$
1.8	60	$1.13 (\pm 0.04) \times 10^{-9}$
2.5	74	$1.60 (\pm 0.02) \times 10^{-9}$

isolation chamber with the lock-in amplifier set for a bandwidth of 1 Hz, which gave an rms value of 0.5  $\mu\text{V}$ . The lock-in amplifier with the microphone switched off gave a noise voltage significantly smaller than this figure. The quality factors for three resonators were determined by varying the laser modulation frequency and electronically recording the output on the lock-in amplifier. The shapes of the acoustic resonances were in accord with the expression for a singly resonant chamber as given in Ref. 10. Table 1 shows the quality factors and detection limits, taken with a 1-s time constant on the lock-in amplifier, based on the experimentally measured absorption coefficient and the intrinsic noise of the microphone for the three resonators that were investigated; detection limits are reported in inverse centimeters per watt as is now customary for photoacoustic detection. For the 1-cm-diameter cell, the calculated detection limit corresponds to 280 parts per million of  $\text{N}_2\text{O}$ , or  $4.7 \times 10^{-5} \text{ cm}^{-1}$ . These two figures could be improved significantly by use of a laser that operated at the absorption maxima of  $\text{N}_2\text{O}$ .

### 3. Discussion

It is now customary to describe the detection limits of a photoacoustic detector in terms of an absorption that is typically given in inverse centimeters. The concentration of a given species at the detection limit is found for the device under consideration by dividing that figure by the extinction coefficient of the species of interest (expressed in inverse moles per liter inverse centimeter) to obtain a minimum concentration that can be detected with a specified signal-to-noise ratio. Furthermore, to describe the effectiveness of a particular acoustic resonator design for trace detection, it is common to factor out the laser power from the detection limit by multiplying the figure for the detection limit in inverse centimeters by the power of the laser in watts used to determine the limit to obtain a quantity with units of inverse centimeters watt. That is, because the photoacoustic effect is typically linear in laser power over a wide range for gases at atmospheric pressure, use of a high-power laser will result in lower detection limits in parts per million than, for example, a low-power laser used with the same resonator; hence the detection limit is normalized to laser power. The smallest value for the detection limit expressed in inverse centimeters watt corresponds to the best resonator irrespective of the laser power and the particular gas used in the experiment to calibrate the device. Table 1 shows that the detection limits reported here for

the internally excited resonator are comparable to those reported for resonators with radially excited modes employing high-power lasers<sup>27</sup> when limits are normalized to laser power. Of course, an improved detection limits as described in inverse centimeters or parts per million can be expected with an increase in average laser power.

Although a rigorous comparison between theory and experiment was not a goal of the experiments reported here, it can be seen from Table 1 that there is qualitative agreement between the results for both the magnitude of the quality factors and the signal amplitude with the theoretical predictions given in Ref. 24 in their dependence on the resonator radius: The quality factor is seen to increase with the radius and the signal amplitude is seen to decrease with an increase in the radius. The trade-off is characteristic for any resonator, with the photoacoustic pressure proportional to the product of the absorbed laser power per unit volume and the cavity  $Q$  when the resonator is driven on resonance. In the present case in which the cavity is cylindrical and the quality factor is proportional to the cell radius, the overall signal, and hence the detection limit, must be inversely proportional to the cell radius.

The present experiments show that an uncooled quantum-cascade laser can be incorporated into the interior of an acoustic resonator, which permits use of the full power of the laser and, with present quantum-cascade laser technology, is the limiting factor in reproducing the low detection limits of conventional photoacoustic trace gas detectors that typically employ low-beam divergence lasers with output powers of the order of 1 W. Further increases in the output power of quantum-cascade lasers should lead to the realization of small, portable detectors useful for trace gas detection at atmospheric pressure, fabricated to be selective for excitation of specific chemical species based on their infrared absorptions.

The authors are grateful for support by the U.S. Office of Naval Research under grant N00014-99-1-1088 and the U.S. Department of Energy under grant ER13235 during the latter stages of this research. The research at Lucent, Inc. was supported in part by the Defense Advanced Research Project Agency and the U.S. Army Research Office under contract DAAD19-00-C-0096.

### References and Note

1. V. E. Gusev and A. A. Karabutov, *Laser Optoacoustics* (American Institute of Physics, New York, 1993), Chap. 2.
2. F. V. Bunkin, Al. A. Kolomensky, and V. G. Mikhalevich, *Lasers in Acoustics* (Harwood, Academic, Reading, Mass. 1991).
3. A. Mandelis, ed., *Progress in Photothermal and Photoacoustic Science and Technology* (Elsevier, New York, 1992), Vol. 1.
4. D. Kliger, *Ultrasensitive Laser Spectroscopy* (Academic, New York, 1983).
5. C. K. N. Patel and A. C. Tam, "Pulsed optoacoustic spectroscopy of matter," *Rev. Mod. Phys.* **53**, 517–550 (1981).
6. E. L. Kerr and J. G. Atwood, "Laser illuminated absorptivity spectrophone: a method for measurement of weak absorptiv-

- ity in gases at laser wavelengths," *Appl. Opt.* **7**, 915–918. (1968).
7. L. B. Kreuzer, "Ultralow gas concentration infrared absorption spectroscopy," *J. Appl. Phys.* **42**, 2934–2943 (1971).
  8. L. B. Kreuzer, N. D. Kenyon, and C. K. N. Patel, "Air pollution: sensitive detection of ten pollutant gases by carbon monoxide and carbon dioxide lasers," *Science* **177**, 347–349 (1972).
  9. J. G. Choi and G. J. Diebold, "A Helmholtz resonator optoacoustic detector for gas chromatography," *Anal. Chem.* **59**, 519–521 (1987).
  10. M. W. Sigrist, ed., *Air Monitoring by Spectroscopic Techniques*, Vol. 127 of Chemical Analysis Series (Wiley, New York, 1994), p. 163.
  11. C. Gmachl, F. Capasso, D. L. Sivco, and A. Y. Cho, "Recent progress in quantum cascade lasers and applications," *Rep. Prog. Phys.* **64**, 1533–1601 (2001).
  12. F. Capasso, C. Gmachl, D. L. Sivco, and A. Y. Cho, "Quantum cascade lasers," *Phys. Today* **55**, 34–40 (2002).
  13. A. A. Kosterev, R. F. Curl, and F. K. Tittel, "Methane concentration and isotopic composition measurements with a mid-infrared quantum-cascade laser," *Opt. Lett.* **24**, 1762–1764 (1999).
  14. J. T. Remillard, D. Uy, W. H. Weber, F. Capasso, C. Gmachl, A. L. Hutchinson, D. L. Sivco, J. N. Baillargeon, and A. Y. Cho, "Sub-Doppler resolution limited Lamb-dip spectroscopy of NO with a quantum cascade distributed feedback laser," *Opt. Exp.* **7**, 243–248 (2000), <http://www.opticsexpress.org>.
  15. B. A. Paldus, C. C. Harb, T. G. Spence, R. N. Zare, C. Gmachl, F. Capasso, D. L. Sivco, J. N. Baillargeon, A. L. Hutchinson, and A. Y. Cho, "Cavity ringdown spectroscopy using mid-infrared quantum-cascade lasers," *Opt. Lett.* **25**, 666–668 (2000).
  16. C. M. Gittins, E. T. Wetjen, C. Gmachl, F. Capasso, A. L. Hutchinson, D. L. Sivco, J. N. Baillargeon, and A. Y. Cho, "Quantitative gas sensing by backscatter-absorption measurements of a pseudorandom code modulated quantum cascade laser," *Opt. Lett.* **25**, 1162–1164 (2000).
  17. A. A. Kosterev, A. L. Malinovsky, F. K. Tittel, C. Gmachl, F. Capasso, D. L. Sivco, J. N. Baillargeon, A. L. Hutchinson, and A. Y. Cho, "Cavity ringdown spectroscopic detection of nitric oxide with a continuous-wave quantum-cascade laser," *Appl. Opt.* **40**, 5522–5529 (2001).
  18. B. A. Paldus, T. G. Spence, R. N. Zare, J. Oomens, F. J. M. Harren, D. H. Parker, C. Gmachl, F. Capasso, D. L. Sivco, N. J. Baillargeon, A. L. Hutchinson, and A. Y. Cho, "Photoacoustic spectroscopy using quantum-cascade lasers," *Opt. Lett.* **24**, 178–180 (1999).
  19. A. Karbach and P. Hess, "High precision acoustic spectroscopy by laser excitation of resonator modes," *J. Chem. Phys.* **83**, 1075–1084 (1985).
  20. A. Karbach and P. Hess, "Photoacoustic signal in a cylindrical resonator: theory and laser experiments for CH<sub>4</sub> and C<sub>2</sub>H<sub>6</sub>," *J. Chem. Phys.* **84**, 2945–2952 (1985).
  21. G. Busse and D. Herboeck, "Differential Helmholtz resonator as an optoacoustic detector," *Appl. Opt.* **18**, 3959–3961 (1979).
  22. J. Pelzl, K. Klein, and O. Nordaus, "Extended Helmholtz resonator in low-temperature photoacoustic spectroscopy," *Appl. Opt.* **21**, 94–99 (1982).
  23. A. Miklos and A. Lorinez, "Windowless resonant acoustic chamber for laser-photoacoustic applications," *Appl. Phys. B* **48**, 213–218 (1989).
  24. S. Bernegger and M. W. Sigrist, "Longitudinal resonant spectrophone for CO laser photoacoustic spectroscopy," *Appl. Phys. B* **44**, 125–132 (1987).
  25. F. G. C. Bijnen, J. Reuss, and F. H. M. Harren, "Geometrical optimization of a longitudinal resonant photoacoustic cell for sensitive and fast trace gas detection," *Rev. Sci. Instrum.* **67**, 2914–2923 (1996).
  26. The limiting theoretical sensitivity of a microphone is determined by thermal fluctuations in the position of the membrane. In practice, the noise introduced by the first amplifier stage is often greater than the thermal noise in the membrane position. For the purposes of this experiment, the noise measured in the microphone is taken to determine the detection limit, irrespective of whether the microphone achieves the thermal noise limit.
  27. V. P. Zharov and V. S. Letokhov, *Laser Optoacoustic Spectroscopy* (Springer-Verlag, New York, 1986), see Table 5.3.